Princeton Plasma Physics Laboratory

PPPL- 4305

PPPL- 4305

Mini-Conference on the First Microns of the First Wall

D.P. Stotler, T.D. Rognlien and S.I. Krasheninnikov

March 2008

Prepared for the U.S. Department of Energy under Contract DE-AC02-76CH03073.

Princeton Plasma Physics Laboratory
Report Disclaimers

Full Legal Disclaimer

Trademark Disclaimer

PPPL Report Availability

Princeton Plasma Physics Laboratory:

http://www.pppl.gov/techreports.cfm

Office of Scientific and Technical Information (OSTI):

http://www.osti.gov/bridge

Related Links:

U.S. Department of Energy

Office of Scientific and Technical Information

Fusion Links

Mini-Conference on the First Microns of the First Wall

D. P. Stotler

Princeton Plasma Physics Laboratory

Princeton University

Princeton, New Jersey 08543

T. D. Rognlien

Lawrence Livermore National Laboratory

Livermore CA, 94551

S. I. Krasheninnikov

University of California at San Diego

La Jolla, CA 92093

(Dated: 12th March 2008)

Abstract

Interactions between plasmas and their surrounding materials (plasma facing components) are of great interest to present and future magnetic fusion experiments, and ITER [ITER Physics Basis Editors, ITER Physics Exper Group Chairs, ITER Joint Central Team, and Physics Integration Unit, Nucl. Fusion **39**, 2137 (1999)] in particular. This interest is the result of concerns with the survivability of these materials, as well as the impact of these interactions back on the plasma. These interactions begin on the surface, but can have consequences a few microns into the material.This mini-conference on these "first microns" was designed to bring to the Division of Plasma Physics Meeting experts on these topics who would otherwise not attend. At the same time, the mini-conference was intended to expose the broader fusion community to these issues. The mini-conference covered in three, half-day sessions the topics of lithium coatings and surfaces, mixed materials characteristics, and issues associated with graphite.

I. INTRODUCTION

Processes occurring at the surface of the material wall surrounding magnetic fusion devices have frequently played a crucial role in the experiments' energy confinement (i.e., performance)[1]. Examples are: the introduction of low-Z limiters to reduce plasma-wall interactions and overcome the impurity radiation barrier; the usage of conditioning discharges and coating techniques such as boronization to attain large increases in plasma temperature; and the injection of lithium that dramatically increased the performance of the last shots[2] of the Tokamak Fusion Test Reactor[3] (TFTR). In spite of these readily acknowledged experimental achievements, researchers have developed only a limited understanding of multi-material interactions (especially important given ITER's choice of beryllium, carbon, and tungsten[4,5]), tritium retention, film deposition and dust formation, etc. Moreover, the available information is largely an empirical "how to" recipe and is not based on a thorough understanding of the underlying physics that can be confidently projected to other devices.

Meanwhile, within the materials science community first principles models of surface physics have been made practical by the rapid increases in computational power and associated scientific and algorithmic improvements over the last decade. The resulting simulation codes can describe the response and evolution of materials to plasma bombardment at a variety of length and time scales, down to those of the atoms themselves (see, for example, Ref. 6 and other papers presented at that workshop). At the same time, experimental techniques for characterizing these processes have continued to improve in accuracy. The talks presented at this mini-conference, combined with the separate tutorial talk by Professor Nasr Ghoniem, provided an opportunity for the broader fusion community to learn about this important topic.

The mini-conference consisted of three half-day sessions, each with roughly 7 20-minute talks covering lithium surfaces and coatings, mixed materials characteristics, and issues associated with graphite and other materials.

II. LITHIUM COATINGS AND SURFACES

The fusion community has long contemplated the use of lithium for conditioning in-vessel tiles or as a plasma facing material. The ability of lithium to absorb hydrogen atoms is usually a prime consideration in these applications. Lithium coatings are also known to getter oxygen and to reduce impurity influxes into the plasma. These combined characteristics are believed to be largely responsible for the tremendous improvements in confinement seen in TFTR's lithium coating experiments[2]. Liquid lithium is also being considered as a primary plasma facing component because of its ability to "self heal" and to absorb high heat fluxes (in addition to its absorption properties). The liquid lithium experiments[7] on the Current Drive Experiment-Upgrade[8] (CDX-U) device are but one example of this pursuit of lithium plasma facing surfaces.

Numerous other presentations at this Division of Plasma Physics meeting described lithium coating experiments carried out on the National Spherical Torus Experiment[9] (NSTX). These coatings were deposited with a single evaporator (LIThium EvaporatoR, or LiTER) inserted at the top of the vessel. The procedure and subsequent plasma results from the 2006 and 2007 NSTX run campaigns were the focus of an invited presentation by H. W. Kugel. The first four talks in this mini-conference session were directly associated with these experiments. The other three addressed more general issues associated with these experiments and with others planned for the future.

W. R. Wampler (Sandia National Laboratories) described analyses of lithium and deuterium concentration versus depth in carbon tiles removed from NSTX after operation with lithium evaporation. Tiles used in the the 2006 and 2007 campaigns were taken from various locations around the torus. For the 2006 campaign tiles, the lithium surface concentration was found to vary between 10^{17} and 5×10^{18} atoms per cm^2, compared with 10^{18} – 10^{19} atoms per cm^2 for tiles from 2007; the higher concentrations in the 2007 tiles are consistent with the larger evaporation rates used then. In both cases, the lithium was confined to within 5 microns of the surface everywhere, suggesting limited diffusion of the lithium into the graphite. Deuterium atom concentrations ranged from 10^{17} – 10^{19} atoms per cm^2 (concentrations in 2007 were slightly lower), all within 4 microns of the surface. In the 2006 campaign, shadowing of tiles by the center stack during evaporation resulted in lithium concentrations about 10% of those in unshadowed regions at similar poloidal locations. However, the deuterium

concentrations in shadowed and unshadowed regions were comparable, indicating that the deuterium concentration was not significantly affected by the lithium coatings. The effect of the shadowing was reduced in the 2007 campaign, presumably due to operation of LiTER during helium glow discharge cleaning.

L. E. Zakharov (Princeton Plasma Physics Laboratory) presented modeling of the LiTER evaporator used during the 2006 NSTX campaign. This work utilized a detailed 3-D model of the internal structure of the evaporator, as well as of each individual tile inside NSTX. An integral technique[10] valid in the limit of lithium atom mean free paths longer than relevant distances was employed, making the calculations very efficient in comparison with Monte Carlo approaches. The model was able to qualitatively reproduce deposition profiles obtained in laboratory tests of the evaporator. The simulated coating thicknesses in NSTX were compared with those obtained from the analysis of silicon coupons and graphite tiles from NSTX at the end of the run campaign (described in the previous talk by Wampler). While the patterns of shadowed regions matched well, the distributions in un-shadowed areas differed in detail. The suspicion is that this discrepancy reflects erosion and redeposition by the plasma. Simulations indicate that this sort of lithium evaporation is useful for passivating water remaining in the graphite tiles. The desired degree of core plasma density control could then be obtained via pumping by a liquid lithium tray in the NSTX divertor.

J. R. Timberlake (Princeton Plasma Physics Laboratory) described simple chemical analyses, electron microscopy, and energy dispersive X-ray spectroscopy of lithium deposits taken from NSTX after the 2007 run campaign. Thick deposits of lithium compounds that had formed near the evaporator's output aperture were tested with litmus paper and immersion in water (after exposure to air in the collection process). The results were consistent with the deposits consisting of lithium particles embedded within lithium hydroxide. In particular, there were no indications of the presence of lithium carbide, leading to the inference that the lithium here was not reacting directly with the graphite tiles. Electron microscopy of the coatings showed a similar morphology of coatings on graphite and gold coated quartz crystals, but a different morphology of coatings on polished silicon coupons (Fig. 1), revealing the influence of the substrate on the coating morphology. Energy dispersive analysis also showed that the trace metals found in the lithium coatings from NSTX did not originate in the evaporator.

C. Skinner (Princeton Plasma Physics Laboratory) discussed measurements of mass de-

position in NSTX, during lithium conditioning and in general, using quartz crystal microbalances (QMB's). The key feature of the QMB as a material diagnostic is that it provides time resolved data at a particular location; one limitation is that this location must be in a low heat flux region to avoid damage to the QMB. Two QMB's operated continuously over a several month long campaign in NSTX showed that for a given shot the deposited mass increases rapidly and then slowly decays. However, the step-up on the first shot of the day is larger than that of subsequent shots by far[11]. At the end of the run day, the deposited mass decays over several hours. These observations are consistent with the mass increases being predominantly due to dynamic retention. In the scenario described by Skinner, deuterium outgasses from the graphite tiles overnight[12]. On the first shot of the day, the surface layers are rapidly resaturated. They outgas immediately between shots, but only partially. It's for this reason that the mass gain between shots is much smaller than that observed on the first shot of the day. The rate of mass loss seen at the end of the day is consistent with this picture if the fraction of the vacuum vessel area subject to dynamic retention is relatively small. An examination of the QMB signals during lithium evaporation by the LiTER device showed a reduced deposition rate during helium glow discharge cleaning, presumably caused by collisions of evaporated lithium atoms with helium or by ionization of the lithium. Skinner also noted occasional sharp drops in the QMB mass at apparently random times and interpreted this as flaking or peeling of the deposited layer attached to the crystal's surface.

J. P. Allain (Purdue University) presented laboratory characterizations of lithiated surfaces, including their response to plasma bombardment and the results of chemical and elemental analyses. Deuterium, helium and lithium atoms (or ions) incident at energies between 50 eV and 5 keV will implant between 5 and 200 nm into a lithium surface. Deuterium atoms in liquid lithium at temperatures higher than 300 - 400° C can diffuse readily, resulting in an effective pumping region that is 250 nm deep[13]. In contrast, particles sputtered from the surface come from within the first 2 - 3 monolayers[14]. The sputtering rate does not depend on whether or not the lithium is liquid unless the surface temperature is more than 50% above the melting point, in which case the sputtering rate greatly exceeds that due to evaporation[15]. If the lithium is saturated with deuterium, deuterium atoms are preferentially sputtered, resulting in a 40% reduction in the lithium sputtering rate[16]. X-ray photoelectron spectroscopy (XPS) analysis of lithium coatings carried out on the Interaction of Materials with Particles and Components[17] (IMPACT) facility at Argonne are unique in

that samples can be analyzed in real time during lithium deposition and without exposure to air (in contrast to the work described above by Wampler and Timberlake). Analysis of graphite tiles from NSTX showed the presence of lithium carbonate, consistent with the lithium coated tiles having been exposed to air. But, lithium carbonate was not seen when graphite samples were coated with lithium in-situ. Instead, lithium peroxide was found, forming very quickly after deposition in spite of the high vacuum, with the oxygen presumably coming from the graphite itself. Subsequent exposure of these samples to air showed the lithium peroxide disappearing over about an hour and the presence of lithium carbonate increasing. Lithium hydroxide may also be present in the samples exposed to air.

M. Racic (University of Illinois at Urbana-Champaign) described measurements of physical sputtering of lithiated graphite surfaces performed on the Ion-surface InterAction eXperiment[18] (IIAX). The deuterium molecular ion (D_2^+) was used as the projectile for these experiments with incident energies of 200 eV/D and 500 eV/D. The amount of mass sputtered from the target is determined with a QMB. This can be converted into a sputtering yield (i.e., number of sputtered atoms per incident ion) if the composition of the sputtered material is known. For pure lithium and graphite (Union Carbide, type ATJ) targets, the sputtered material is assumed to consist entirely of lithium and carbon, respectively. The resulting sputtering yields match well those computed by the Transport of Ions in Matter[19] (TRIM) code. But, for ATJ tiles coated with lithium in situ (at thicknesses of 150 and 300 nm, assuming equal numbers of lithium and carbon atoms in the sputtered material), the sputtering yields were $\sim 20\%$ of those found with pure lithium (Fig. 2). The inferred conclusion is that the lithium is forming surface or near-surface compounds with the graphite, resulting in a reduced sputtering rate. But, at the same time it impairs the pumping ability of the coatings. This is consistent with the NSTX observations of a limited duration for the beneficial effects of lithium evaporation.

M. A. Jaworski (University of Illinois at Urbana-Champaign) discussed the motion of liquid lithium under applied heat loads. The particular situation considered for this work was the Liquid Lithium Divertor (LLD) planned for installation on NSTX in FY-2009. The baseline configuration of the LLD is of a porous molybdenum mesh soaked with liquid lithium. Surface tension and viscous effects should limit the macroscopic motion of liquid lithium in this case. In particular, thermocapillary (Marangoni) flows[7] are not expected to be significant. Without any such flows and under NSTX relevant heat fluxes, evaporative cooling will

not be sufficient to keep the liquid lithium at a constant temperature. Hence, evaporation strong enough to influence the divertor plasma is anticipated, perhaps resulting in divertor detachment. The possible impact of thermoelectric effects[20] on the LLD were also examined. Estimates suggest that these effects could impair the ability of the liquid lithium to flow to the top of the porous mesh where it would be needed to replace evaporated material. The Solid/Liquid Lithium Divertor Experiment (SLiDE) being built at the University of Illinois will study this and other effects more thoroughly.

III. CHARACTERISTICS OF MIXED MATERIALS

The use of different materials for various plasma-facing components (e.g., divertor plate, baffles, and main-chamber wall) substantially complicates the understanding of the surface layer that forms owing to material erosion, transport within the edge plasma, and final redeposition on a remote surface. Such considerations are of great current interest as the ITER design calls for carbon divertor plates, nearby tungsten baffles, and a beryllium main-chamber wall for the initial physics phase. It is important to understand the maximum heat flux such materials can withstand and their sputtering yields in a fusion plasma environment. In addition, the ability to predict the amount of hydrogen isotopes that can be retained in these materials, as well as a means to periodically remove the same, is a key issue for fusion devices where safety regulations limit the amount of tritium that can reside in the walls.

J. Hanna (University of California at San Diego) described a set of results from the linear PISCES-B[21] experimental device with an axial magnetic field that approximates plasma conditions in the divertor region of a tokamak discharge. PISCES-B operates within an overall safety enclosure that prevents release of any material, thereby making the device ideally suited to study beryllium (Be) interactions with carbon (C) and tungsten (W) surfaces in a plasma discharge. This presentation focused on Be/C interactions, and the following presentation by Baldwin considered Be/W mixtures. At one end of the device, the plasma is terminated by a sample of C, and the Be is introduced as a gas along a portion of the radial wall from an oven whose temperature controls the magnitude of the evaporative Be flux onto the hydrogen, deuterium, or helium plasma column. Electron and ion energies are similar to that expected in the divertor of ITER, while the electron density and confining magnetic field are typically substantially smaller. In addition to steady-state plasma con-

ditions, the effect of transients in the plasma energy flux to a sample divertor surface from Edge Localized Modes (ELM) in tokamaks is simulated in PISCES-B by biasing the sample with a fast pulse network yielding a minimum width of $\sim$ 10ms.

The key Be/C results reviewed by Hanna are as follows: a Be concentration within the plasma as small as 0.2% compared to deuterium is sufficient to strongly suppress carbon erosion for the end plates as measured by CD and C emission. X-ray photoelectron spectroscopy of the plate surface confirms the formation of a carbidic layer of C, which mitigates C chemical erosion[22]. The time constant for the reduction of C erosion is fit by a simple empirical formula that includes variations of plasma flux, ion energy, and surface temperature; the time constant is typically many seconds[23]. Increased surface temperature during the ELM simulation is found to give the lower range of the time constant[24,25]. It is also found that deuterium retention for a pure Be_2C surface is $\sim$ 2 times larger compared to a C surface, and that both decrease about an order of magnitude from $\sim 50^\circ$ to $\sim 400^\circ$ C and then decrease much more slowly[26].

M. J. Baldwin (University of California at San Diego) then presented result from PISCES-B on Be/W, where W inserted into the sample holder at one end. Because a fusion plasma will contain helium (He), there is interest in understanding previous observations of bubble and blister formation and surface nano-structures for a W surface exposed to a He plasma[26–28]. Thus, this presentation concentrated on the properties of the nano-structures observed on W plates in PISCES-B exposed to an He plasma discharge (Fig. 3) and reported the effect of Be gas injection. Without Be, the W nano-structure complex (having many voids) beyond the surface can grow to $\sim$ 1 μm with a negligible weight loss/gain of the W target. At this size, there is a question of if the He plasma can interact with the solid W surface, but the structures do continue to grow (hot W immersed in He gas do not grow these structures). The growth of the nano- structures obeys a simple diffusion modeling yielding a thickness that increases as $t^{1/2}$, where t is time, and the rate increases with surface temperature; little sensitivity to plasma flux is observed. Introduction of as little as 0.1-0.2% Be ions to the plasma significantly reduces the growth of the nano-structures, either in a dominantly He plasma or a D plasma with 10% He ions. The measured growth of the Be layer on the surface can be fit by a simple rate model including reflection, sputtering, redeposition, evaporation, and bulk diffusion. At a surface temperature of $\sim$ 1150 K, is found that formation of either a Be layer of a C layer is sufficient to suppress growth of

the nano-structures. The initial overall conclusion related to ITER are that with the initial C/W/Be design and a surface temperature less than 1000 K, nano-structure formation will likely not occur. However, for an all-W divertor and baffle devices, both non- structures and BeW alloy layers may form if the surface temperature is greater than 1000 K.

J. N. Brooks (Argonne National Laboratory) reported on models used to simulate the erosion of wall materials, ionization and transport in the edge plasma, and redeposition at a different surface location. A variety of codes were used to model different aspects of the problem. The focus was simulations of mixed material transport for ITER conditions and comparing different combinations of plasma facing component (PFC) materials as reported in Ref. 29. The basic hydrogenic (deuterium/tritium) plasma solution was obtained from the 2D UEDGE[30] transport code including a strong outward plasma convection in the scrape-off layer to describe rapid "blob" filamentary transport observed in a number of devices. The sputtering caused by the hydrogenic wall flux is then evaluated by the 3D WBC Monte Carlo code[31] for impurities from either a Be or W wall, which are followed into the plasma until deposited on another surfaces as ions and perhaps re-sputtered. For normal operation, the calculation predicts that about 1 cm of Be would erode for Be and only 0.006 cm for a W wall, both giving acceptable values of core impurity contamination; the impact of ELMs and disruptions was not modeled. The surface interaction of the sputtered Be followed by WBC onto a carbon divertor was modeled with the SIBIDET wall code[32] that includes surface physics and time-dependent1D transport of Be into the carbon.

D. G. Whyte (Massachusetts Institute of Technology) discussed experiments in the Alcator C-Mod tokamak[33] hydrogen retention molybdenum (Mo), a refractory metal, and corresponding modeling interpretation of the results. Historically, it has been believed that refractory materials would have a substantially lower hydrogen (H) inventory than carbon because the much lower intrinsic solubility of H, in spite of the metal's higher permeability to H. However, experimental results, both from overall C-Mod particle balance followed over many discharges and from in-situ depth profiling of H in Mo sample using the Dynamics of ION Implantation and Sputtering of Surfaces (DIONISOS) diagnostic device[34], indicate retention is non-trivial in Mo. In C-Mod, the Mo surface is boronized periodically, which acts as a permeation barrier to prevent significant uptake of H in the Mo. However, it is found there is a continual net uptake of H over a number of discharges. The developing understanding of this results is that some areas on the outer divertor are found to have the

boron eroded away well before the next boronization, and the amount of retention is best correlated with H ion flux to this region. Even given this bare-Mo explanation, the net H retention substantially exceeds the expectation based on a clean Mo surface[35]. The DION-ISOS lab experiments on a Mo sample provide a reason for this larger-than-expect retention, where two mechanisms are identified[36]. The first is that H release from the surface depends on recombination with another H atom to be released as H_2; thus during high plasma fluxes the surface can become super-saturated, which drives a high flux into the material, but when the discharge is terminated, the surface H drops quickly, and the injected H has a harder time finding a surface H partner to escape with such that the preferred transport direction is inward. Secondly, high plasma energy flux (or neutrons in ITER) produces damage and localized H traps that can retain large amounts of H. These traps are mobile, can diffuse inward, and become frozen into cold walls after a discharge. The net result is a ratio of D/Mo deep in the material that can approach 1%, much larger than predicted by previous analyses. This result suggests that use of a wall temperature significantly higher than the planned 150° C, or transient wall heating in ITER, might be needed to control the H (T) inventory for refractory metal PFCs.

A. A. Haasz (University of Toronto) reviewed results on the removal of D from carbon tiles taken from the DIII-D[37] and JET[38] tokamaks using the thermo-oxidative technique (Fig. 4)[39–41]. These tiles had redeposited layers of combined D and C material after many plasma discharges. The DIII-D samples had relatively thin layers of about 2 μm that contained less than 5% boron from periodic boronizations. The D removal technique subjects the samples heated to various temperatures ($T_s \sim 523$ – 673 K) to O_2 gas at different pressures ($p \sim 0.21$–79 kPa). The results show that as T_s and O_2 pressure are increased, the initial removal rate increases, while the final D content decreases[40,41]. More than 85% of the D content can be removed in 2 hours for $T_s = 623$ K and $p > 20$ kPa from DIII-D codeposits with a few percent B concentration. The amount of D remaining in the codeposit after oxidation increases with increasing B content. For the JET tiles, the co-deposited D/C layer was much thicker, from 10-250 μm, and instead of B, Be was the main impurity with Be/C ratios as high as unity. The D content [D/(Be+C))] varied from 0.8 in shadowed areas to $\sim 0.1 - 0.2$ elsewhere. Here oxidative D removal was performed at $T_s = 623$ K and the O_2 pressure of $p = 21$ kPa. About 90% of the D was removed in less than 2 hours. The initial removal rate varied linearly with the original D content of the codeposit, and > 85%

of the original D content was removed after 8 hrs. of oxidation, independent of the inherent Be content and codeposit thickness[41]. The noted difference in the effect of B and Be on the oxidative removal of D from DIII-D and JET codeposits is not yet explained. The JET results projected to ITER give that more than 90% of the D (T) could be removed in 1 day for $T_s \sim 350^\circ$ C and $p > 21$ kPa.

C. P. C. Wong (General Atomics) presented a new concept for a PFC that could support the necessary heat-handling capability as well as avoiding other problems such as radiation damage from helium ions to the W surface. This mixed-material concept utilizes a ~ 2 mm thick tungsten mesh that is infiltrated and covered with B; about 50% of the mesh volume would be composed of voids. The goal is to maintain a sufficient coverage of B to protect the W from transient damage by ELM's and disruptions, while at the same time being able to utilize the high thermal conductivity of W to rapidly carry away the excess heat through the combined porous medium. There are many issues that need to be resolved to show that his concept is viable in a steady state tokamak. Erosion of B will be high. The B layer will need to be replenished via in-situ boronization. Experiments have shown that trapped hydrogen can be released at $\sim 400^\circ$ C from a pure B layer. To reduce neutron absorption from B, isotopic tailoring with the use of ^{11}B is needed. Key questions on the handing of ELMs and disruption, and in-situ re-coating of B could be explored in present-day devices such as the Divertor Material Evaluation Studies[42] (DiMES) or Midplane Material Evaluation Studies[43] (MiMES) probes in DIII-D.

Y. W. Kim (Lehigh University) discussed the basis of a physical model to predict the elemental composition profile of a multi-element alloy specimen under influence of an imposed gradient field, such as by a rapid change in the surface temperature or by an incoming flux of energetic particles; both types occur in PFCs for fusion devices. The composition affects such basic quantities as thermal and electrical conductivities. He also described a laboratory diagnostic system based on time-resolved spectroscopy of a surface plasma plume created by laser irradiation of a material specimen used in order to measure the evolution of near-surface composition profile[44]. The model is based on the observation that a non-crystalline material specimen consists of random close-packed atoms of constituent species. As such, the specimen is morphologically a mixture of glassy matter and nano-crystallites. When the specimen temperature is raised either due to thermal conduction, electrical current or by incident energetic particles, nano-crystallites undergo melting while atom fluctuations in-

crease. The thermal (or electric) fields, or concentration gradients, enhance atom transport, resulting in changes in morphology. The size distribution, of nano-crystallites can be measured or modeled after the mechanism of nano-particle formation in an atom vapor plume[45]. The melting of nano-crystallites can be treated by means of the law of mass action. Fluctuating atoms in a metallic alloy environment are further attracted to the surface by their image fields. Examples of these techniques applied to nichrome specimens were given, and it was suggested that the same analysis could help understand the fundamental properties of mixed-materials in fusion devices.

A. S. Kukushkin (ITER) presented a series of calculations to estimate the buildup rate of hydrocarbon co-deposits in the small gaps between individual wall tiles that would contribute to the tritium inventory in the ITER device. The hydrogenic and carbon fluxes (ions and neutrals) to the walls are taken from ITER edge-plasma simulations using the B2-EIRENE 2D transport code[46]. The simulations allow for the deposition of carbon on initially non-carbon surfaces such as the Be first wall, and for re-erosion of these deposits. If the carbon flux onto a local wall region exceeds the erosion (mostly via chemical sputtering), even the initially Be wall is assumed to have a normal carbon surface. Assuming the chemical erosion yield Y_{ch} for the deposited carbon on the first wall is an order of magnitude higher that for the original carbon surface on the targets, it is found that no net carbon deposition is expected on the front surfaces of the first wall tiles[47]. The analysis then considers the accumulation of co- deposited hydrocarbons in the gaps between these tiles. It is shown that the flux dependence of Y_{ch}[48] may lead to a carbon deposition in the gaps even when the front surface is clean, and that the deposition pattern may be non-monotonic. According to deposition–re-erosion conditions, the gaps are divided into different zones (Fig. 5) away from the surface facing the plasma: the first has line-of-sight contact with streaming plasma along the tilted magnetic field line (zone 1), the second is a region where re- sputtered hydrocarbons can diffuse more deeply via multiple "reflections" off the gap walls (zone 2), and the final section is where the downward moving hydrocarbons are mostly deposited (below zone 2). A parameter in determining the buildup is the ratio of the depth of the line-of-sight gap region to the width of the gap, although results are not too sensitive to this ratio. For ITER, the estimates are that the co-deposition of T in the gaps is below 0.2 gm/discharge, such that several thousand discharges could be performed without reaching the T safety limit, if this were the only mechanism of the co-deposition. Furthermore, if the carbon re-eroded from

the chamber wall does not recycle locally, the net accumulation would be substantially less.

IV. GRAPHITE WALL SPUTTERING AND EVOLUTION

Carbon, so far, has been widely used as a first wall material in fusion research, and, as projected, will be used in ITER as a material for the divertor targets. However, the main problems with carbon as a candidate for the first wall material, are high erosion and tritium retention. In addition to the graphite-plasma interactions, other issues of plasma interactions with the first wall were considered in this session.

F. W. Meyer (Oak Ridge National Laboratory) discussed chemical sputtering of graphite surfaces by slow H and D atomic and molecular projectiles. Even though both erosion of graphite and retention of the hydrogen in graphite were studied rather extensively, still there are topics where additional research is needed. Especially for low temperatures of plasma (below 10 eV) compatible with detached divertor conditions such issues as the extent of (H, D, T) isotope effect in chemical sputtering, chemical sputtering thresholds, dependence on surface morphology and structure, etc. need additional study. The ORNL apparatus uses decelerated beams with amperes of current of projectiles as low as a few eV in energy. A quadrupole mass spectrometer is used to monitor partial pressure growth of sputtering products due to ion dosing and the absolute sputtering yield is determined with calibrated hydrocarbon leaks. ATJ graphite (polycrystalline) targets at room temperature were used in experiments. While conventional wisdom suggests that the yield of the molecular ion D_n^+ at energy E is equivalent to the yield of n D^+ ions at energy E/n, experiment shows that at the energies below ~ 60 eV/D molecular projectiles result in enhanced chemical sputtering yield per incident D[49], although the mechanism of enhancement is still not clear. Similar molecular size effects were observed also in hydrogen, and the D, H isotope effect ranges from 1 to 1.5, which is consistent with the conclusions from Ref. 50. Future plans include, in particular, study of the impact at elevated target temperatures (400–900 K), which is more relevant for ITER conditions; measurements of the erosion of a-C:D thin films from IPP-Garching; and measurements on metal (W, Ti, V) - doped C films from IPP-Garching.

P. S. Krstic (Oak Ridge National Laboratory) discussed the results of molecular dynamics (MD) simulations of plasma-surface interactions of deuterated carbon. He emphasized the complexity of such a fundamentally multiscale problem as the chemical sputtering of carbon,

where the theory should simultaneously take into account elastic reflection, implantation, trapping/detrapping, and re-emission of particles. Generally, only the combination of MD for fast ∼ps processes (e.g. collisional cascade and sputtering at impact energies for which implantation depth is not larger than a few nm, i.e. a few tens of eV/D), where the equation of motion is solved for each particle, and Monte Carlo (MC) for slow ∼ms transport processes, where MC solves transport equations, can give us a comprehensive picture. The key element of MD is the inter-atomic potential, which usually is a predefined, semi-empirical function and doesn't allow for electronic excitations. He also discussed different approaches to MD ranging from quantum mechanical to quantum-classical MD, where the potential energy of particle interactions is calculated at each time step by solving Schrödinger equation for electrons with adiabatic instantaneous Hamiltonian. Remarkable agreement of the results of the MD simulations (specially prepared to mimic the experimental conditions!) and experimental data from Meyer's Group was claimed[51]. The best agreement is found when in the simulations the impinging H_2 is highly vibrationally excited. Simulations also predict that the ejecta from the damaged surface of carbon are very different from those of the initial surface and more complex hydrocarbons are sputtered with increasing impact energy of the projectile[52]. Moreover, the ro-vibrational energy of sputtered hydrocarbons is significantly larger than that of hydrogenic molecules. Future plans include the simulation of carbon sputtering in plasma environment, analysis of new targets C crystalline, polycrystalline structures, carbon fiber composite (CFC), doped C, tungsten, beryllium, etc.

Yevgeny Raitses (Princeton Plasma Physics Laboratory) discussed structural studies of carbon dust samples exposed to NSTX plasmas. It is well known that all current tokamaks have some amount of dust inside their working chambers. However, dust in ITER, in particular from ITER's graphite divertor tiles, can pose significant safety issues. Possible mechanisms of dust formation include: fragmentation of wall material during abnormal events (e.g. disruptions); flaking of thin films or re-deposited material; volumetric growth during wall cleaning or conditioning. However, different formation mechanisms of carbonaceous dust should leave their signatures in dust macro and micro-structures including Raman spectra. Raman spectroscopy studies suggest that tokamak-produced dust consists of graphite-like particles with different degree of disordering[53]. The main goal of the presented study was to explore plasma and thermal effects on structural modifications of graphite dust particles. Authors compare Raman spectra of dust particles (∼mm size) from deuterium discharge in

NSTX and atmospheric pressure helium arc discharge, vacuum heat treatment (no plasma), and from unused graphite tile. Presented experimental data show that the Raman spectra of cathode soot from arc experiments and NSTX dust samples are similar and demonstrate a strong disordering, while data from heated samples (heating to ∼2000°C) show weak disordering, and arc anode tip and unused graphite tile show a clear graphitic order. The reporter concluded that the production of carbon dust particles in NSTX and arc discharge involves ablation processes with following deposition and the formation of similarly disordered forms of carbon material. Just heating of the samples to temperatures of 2000-2500 °C cannot create such disordering (see Fig. 6 compiled from the Raitses's presentation). The double peaked shape of the Raman spectrum of the NSTX dust and post-arc cathode soot is similar to the results from Tore Supra[54] and JT-60U[55].

A. Yu. Pigarov (University of California at San Diego) discussed the dynamics of hydrogen inventory in the first wall and tokamak main chamber under strong plasma-wall coupling. Sophisticated integrated modeling tools are needed for the assessment, prediction, and control of plasma transport, power load handling, wall erosion and re-deposition processes, migration of eroded material, and tritium retention and transport in wall materials in ITER and in future magnetic fusion reactors. However, so far there is very limited experience in the coupled plasma-wall modeling. For these reasons, the main focus of the work is on the study of synergetic effects in the coupling of particle and energy transport processes in plasma and wall regions. The author reports on newly developed transport code - the Wall and Plasma-Surface Interaction (WallPSI) - to calculate the wall temperature, erosion rates, and concentration of absorbed, mobile and trapped particle species in the wall material. The code incorporates a new approach in the modeling of the release of hydrogen based on the surface directed convection of hydrogen in the implantation stimulated by plasma bombardment. As a first step the hydrogen transport in the wall impacted by plasma at high and low wall temperatures and for various materials (C, Be, W) was simulated. Wall saturation time, wall pumping efficiency, mobile and trapped hydrogen inventories, and permeation properties for different materials and plasma conditions were reported and the role of stimulated convection in wall saturation and in dynamics of chemical erosion was highlighted. Recently, it was suggested[56] that the interactions of plasma with hydrogen-saturated wall can cause thermal instabilities resulting in massive release of gas from walls. More detailed studies of plasma-wall coupling and featured instabilities was performed by using the

WallPSI code coupled to 1-D plasma transport code EDGE1D[57] (which mimics the radial plasma transport in tokamaks by solving equations: for plasma and neutral densities and for electron, ion and neutral temperatures). Preliminary results of the modeling of coupled plasma-wall system show that without external stabilizing loop (e.g., gas puffing/pumping) the evolution can end up with plasma-wall instability resulting in either formation of Multi-faceted Asymmetric Radiation From the Edge (MARFE) or high-temperature low-recycling edge plasma. The WallPSI module is also used in ongoing Scientific Discovery through Advanced Computing (SciDAC) project on Framework Application for Core-Edge Transport Simulations (FACETS). Recent report on the progress toward integrated modeling can be found in Ref. 58.

K. R. Umstadter (University of California at San Diego) reported on the investigation of plasma surface interactions with the PISCES[59] ELM laser system. When an ELM occurs in tokamaks, up to 30% of the pedestal energy can be deposited on the wall of the tokamak causing heating, material loss due to sublimation, evaporation and melt splashing of PFCs and ejection of wall material into the plasma core. Simple estimates indicate that a pulsed laser system can be used to simulate the heat pulse of ELMs. The laser system was integrated recently into PISCES device. An Nd:YAG laser capable of delivering up to 1 J of energy over a several nanosecond pulse width is used for the experiments. Laser heat pulse only, hydrogen/deuterium plasma only, and laser plus plasma experiments were conducted. The initial results indicate that tungsten samples behave very differently while exposed simultaneously to plasma and heat pulses. Synergistic effects between the heat pulse and a deuterium plasma cause greater surface roughening and material removal (see Fig. 7 taken from Umstadter's talk). The enhanced erosion of surfaces at ITER-relevant impact energy is observed. The ablated material is found (using in situ spectroscopy) in the range of mm to several cm in front of surface. Such penetration of ablated material through the plasma is beyond the standard penetration length (on the order of the mean free path) of atoms of ablated material, and it suggests that clusters and nano-particles are part of the ablated material. It is also shown that the threshold for surface damage is lowered, which emphasizes the need for heat pulse testing to be completed during concurrent plasma exposure.

Roger Stoller (Oak Ridge National Laboratory) discussed atomistic simulations of energetic particle interactions with the first wall. Atomistic simulations of the interactions between energetic particles and a fusion reactor first wall have been carried out using molec-

ular dynamics to investigate both primary damage formation in the structural first wall material and the sputtering of surface atoms which can lead to contamination of the plasma. In the case of damage formation in the structural material, the results provide a quantitative measure of the effect of a nearby free surface on the evolution of atomic displacement cascades, and the nature of the residual damage produced. This damage is characterized by the total number of point defects (vacancies and interstitials), as well as the number and size distribution of point defect clusters produced. A sufficient number of simulations have been completed to statistically evaluate variations between surface-influenced and bulk cascades. Surface sputtering from the molecular dynamics simulations is compared to the results obtained with a more simple, and widely-used Monte Carlo model (Stopping and Range of Ions in Matter, SRIM[60]). A substantial database of atomic displacement cascades in iron has been developed[61] that can provide a basis for evaluating the effect of free surfaces. Comparison of MD cascade in simulations conducted for iron at various distances from a free surface demonstrates a systematic effect on primary damage formation: stable vacancy production increases as cascade initiation site approaches surface; stable interstitial production may increase or decrease as cascade initiation site approaches surface (note that the number of vacancies is greater than the number of interstitials); vacancy clustering fraction increases and cluster sizes increase for near-surface cascades; changes in interstitial clustering are more modest for near-surface cascades; sputtering of atoms from structural material observed. The apparent visible "defect yield" will be higher for in-situ irradiation experiments than for bulk neutron irradiation. Future plans, in particular, include application of developed approach to other plasma-facing materials.

Acknowledgments

We thank the mini-conference participants (named in the text) for providing key input, both in the form of their presentations and by helping to edit these summaries of their work. We also wish to acknowledge the assistance of S. Kruger in the planning of the mini-conference, and the advice and support of the other members of the Edge Coordinating

Committee.

---

[1] G. Federici, C. H. Skinner, J. N. Brooks, J. P. Coad, C. Grisolia, A. A. Haasz, A. Hassanein, V. Philipps, C. S. Pitcher, J. Roth, W. R. Wampler, and D. G. Whyte, Nucl. Fusion **41**, 1968 (2001).

[2] D. K. Mansfield, D. W. Johnson, B. Grek, H. W. Kugel, M. G. Bell, R. E. Bell, R. V. Budny, C. E. Bush, E. D. Fredrickson, K. W. Hill, D. L. Jassby, R. J. Maqueda, H. K. Park, A. T. Ramsey, E. J. Synakowski, G. Taylor, G. A. Wurden, Nucl. Fusion **41**, 1823 (2001).

[3] R. J. Hawryluk, Rev. Mod. Phys. **70**, 537 (1998).

[4] ITER Physics Basis Editors, ITER Physics Expert Group Chairs, ITER Joint Central Team, and Physics Integration Unit, Nucl. Fusion **39**, 2137 (1999).

[5] Progress in the ITER Physics Basis Editors, Nucl. Fusion **47**, S1 (2007).

[6] S. J. Stuart, M. T. Knippenberg, O. Kum, and P. S. Krstic, Phys. Scripta **T124**, 58 (2005).

[7] R. Kaita, R. Majeski, T. Gray, H. Kugel, D. Mansfield, J. Spaleta, J. Timberlake, L. Zakharov, R. Doerner, T. Lynch, R. Maingi, and V. Soukhanovskii, Phys. Plasmas **14**, 056111 (2007).

[8] T. Munsat, P. C. Efthimion, B. Jones, R. Kaita, R. Majeski, D. Stutman, and G. Taylor, Phys. Plasmas **9**, 480 (2002).

[9] M. Ono, S. M. Kaye, Y.-K. M. Peng et al., Nucl. Fusion **40**, 3Y 557 (2000).

[10] P. M. Valanju, J. Comp. Phys. **88**, 114 (1990).

[11] C. H. Skinner, H. W. Kugel, A. L. Roquemore, R. Maingi, and W. R. Wampler, J. Nucl. Mater. **363–365**, 247 (2007).

[12] P. Andrew and M. Pick, J. Nucl. Mater. **220–222**, 601 (1995).

[13] J. N. Brooks, J. P. Allain, T. Rognlien, and R. Maingi, J. Nucl. Mater. **337–339**, 1053 (2005).

[14] P. Sigmund, Phys. Rev. **184**, 383 (1969).

[15] J. P. Allain, M. D. Coventry, and D. N. Ruzic, J. Nucl. Mater. **313–316**, 641 (2003).

[16] J. P. Allain and D. N. Ruzic, Nucl. Fusion **42**, 202 (2002).

[17] J. P. Allain, M. Nieto, M. R. Hendricks, P. Plotkin, S. S. Harilal, and A. Hassanein, Rev. Sci. Instrum. **78**, 113105 (2007).

[18] M. D. Coventry, J. P. Allain, and D. N. Ruzic, J. Nucl. Mater. **313–316**, 636 (2003).

[19] D. N. Ruzic, Nucl. Instrum. and Meth. B **47**, 118 (1990).

[20] J. A. Shercliff, J. Fluid Mech. **91**, 231 (1979).

[21] R. P. Doerner, M. J. Baldwin, and K. Schmid, Phys. Scr. **T111**, 75 (2004).

[22] M. J. Baldwin, R.P. Doerner, D. Nishijima, K. Schmid, D. G. Whyte, J. G. Kulpin, and G. Wright, J. Nucl. Mater. **358**, 96 (2006).

[23] D. Nishijima, J.J. Baldwin, R.P. Doerner, and R. Seraydarian, J. Nucl. Mater. **363–365**, 1261 (2007).

[24] J. Hanna, R. Doerner, R. Hernandez, R. Seraydarian, and R. Pugno, Rev. Sci. Inst. **77**, 123503 (2006).

[25] R. Pugno, M.J. Baldwin, R.P. Doerner, J. Hanna, D. Nishijima, and G. Antar, J. Nucl. Mater. **363–365**, 1277 (2007).

[26] W. M. Shu, G.-N. Luo, and T. Yamanishi, J. Nucl. Mater. **367–370** (2007).

[27] D. Nishijima, M.Y. Yu, N. Ohno, and S. Takamura, J. Nucl. Mater. **313–316**, 97 (2003).

[28] M. J. Baldwin and R. P. Doerner, Nucl. Fusion **48**, 035001 (2008).

[29] J. N. Brooks, J.P. Allain, and T.D. Rognlien, Phys. Plasmas **13**, 122502 (2006).

[30] T. D. Rognlien, J. L. Milovich, M. E. Rensink, and G. D. Porter, J. Nucl. Mater. **196**, 347 (1992).

[31] J. N. Brooks, Fus. Eng. Design **60**, 515 (2002).

[32] J. P. Allan, A. Hassanein, M. Nieto et al., in *Emerging Lithographic Technologies IX*, Proceedings of the Society of Photo-Optical Instrumentation Engineers, Volume 5751, p. 1110, San Jose, California, (2005), edited by R. S. Mackay.

[33] I. H. Hutchinson, R. Boivin, F. Bombarda et al., Phys. Plasmas **1**, 1511 (1994).

[34] G. M. Wright, D. G. Whyte, B. Lipschultz, R. P. Doerner, and J. G. Kulpin, J. Nucl. Mater. **363–365**, 977 (2007).

[35] B. Lipschultz, Y. Lin, M.L. Reinke et al. Phys. Plasmas **13**, 056117 (2006).

[36] D. G. Whyte, "Hydrogenic fuel recovery and retention with metallic plasma-facing walls in Alcator C-Mod tokamak," 21st IAEA Fusion Energy Conference, 16-21 October, 2006, Chengdu, China (2006) EX/P4-29.

[37] J. L. Luxon, Nucl. Fusion **42**, 614 (2002).

[38] JET Team, Nucl. Fusion **45**, S118 (2005).

[39] A. A. Haasz, C.K. Tsui, J.W. Davis, and R. Ochoukov, Phys. Scr. **T128**, 55 (2007).

[40] R. Ochoukov, A.A. Haasz, and J.W. Davis, Phys. Scr. **T124**, 27 (2006).

[41] C. K. Tsui, A.A. Haasz, J.W. Davis, J.P. Coad, and J. Likonen, Nucl. Fusion **48**, 035008 (2008).

[42] A. G. McLean, J. W. Davis, P. C. Stangeby et al., J. Nucl. Mater. **363–365**, 86 (2007).

[43] C. P. C. Wong, D. L. Rudakov, J. P. Allain et al., J. Nucl. Mater. **363–365**, 277 (2007).

[44] Y. W. Kim, Int. J. Thermophysics **28**, 732 (2007).

[45] Y. W. Kim, H.-D. Lee and P.A. Belony, Jr., Rev. Sci. Instr. **17**, 10F115 (2006).

[46] A. S. Kukushkin, H. D. Pacher, V. Kotov, D. Reiter, D. P. Coster, and G. W. Pacher, J. Nucl. Mater. **363–365**, 308 (2007).

[47] A. S. Kukushkin, H.D. Pacher, D.P. Coster, G. W. Pacher, and D. Reiter, J. Nucl. Mater. **337-339**, 50 (2005).

[48] J. Roth, A. Kirschner, W. Bohmeyer et al., J. Nucl. Mater. **337-339**, 970 (2005).

[49] L. I. Vergara, F. W. Meyer, H. F. Krause, P. Träskelin, K. Nordlund, and E. Salonen, J. Nucl. Mater. **357**, 9 (2006).

[50] A. A. Haasz and J. W. Davis, Fusion Sci. Technol. **50**, 58 (2006).

[51] F. W. Meyer, P. S. Krstic, L. I. Vergara, H. F. Krause, C. O. Reinhold, and S. J. Stuart, Phys. Scr. **T128**, 50 (2007).

[52] P. S. Krstic, C. O. Reinhold, and S. J. Stuart, New J. Phys. **9**, 209 (2007); ibid EuroPhysics Letters **77**, 33002 (2007).

[53] P. Roubin, C. Martin, C. Arnas, Ph. Colomban, B. Pégourié, and C. Brosset, J. Nucl. Mater. **337–339**, 990 (2005).

[54] J. Jacquinot, Nucl. Fusion **45**, S118 (2005).

[55] K. Ushigusa and the JT-60 Team, in *proceedings of the 16th IAEA Fusion Energy Conference*, Montreal, Canada (International Atomic Energy Agency, Vienna, 1997), Vol. 1, p. 37.

[56] S. I. Krasheninnikov and T. K. Soboleva, Phys. Plasmas **13**, 094502 (2006).

[57] R. Simonini, A. Taroni, M. Keilhacker, G. Radford, J. Spence, G. Vlases, M. L. Watkins, and S. Weber, J. Nucl. Mater. **196–198**, 369 (1992).

[58] J. R. Cary, J. Candy, R. H. Cohen et al., Journal of Physics: Conference Series **78**, 012086 (2007).

[59] D. M. Goebel, G. Campbell, and R. W. Conn, J. Nucl. Mater. **121**, 27 (1984).

[60] J. F. Ziegler, J. P. Biersack, and U. Littmark, *Stopping and Range of Ions in Matter* (Pergamon Press, New York, 1985).

[61] R. E. Stoller and A. F. Calder, J. Nucl. Mater., **283**, 746 (2000).

Figure captions

1. (Color online) Electron micrographs of lithium coatings on (a) gold (from NSTX), (b) silicon (as deposited in the laboratory), and (c) graphite (also in the lab). All are at a magnification of 265× (from the talk by J. R. Timberlake).

2. (Color online) Comparison of the sputtering yield as measured on the IIAX device with TRIM simulations over a range of incident ion energies. The TRIM results for deuterium incident on pure ATJ graphite and lithium are shown, as are the corresponding measurements (the yield is computed with the assumption that the sputtered material is composed entirely of carbon and lithium atoms in the respective instances). These yields are all much larger than the measured yields obtained with deuterium incident on graphite with three different lithium coatings, assuming equal numbers of lithium and carbon atoms in the sputtered material (from the talk by M. Racic).

3. Filamentary nano-structures that develop on the surface of tungsten when exposed to a helium plasma in PISCES for 4.3×10^3 s. The total height of the structure is $\sim 1\ \mu$m. Energy dispersive x-ray microanalysis shows that the near-surface region A and more distant region B are both predominantly composed of tungsten (from Ref. 28 with permission).

4. (Color online) Remaining deuterium (D) content in carbon divertor tiles taken from DIII-D following exposure to O_2 at various pressures and tile temperatures (from Ref. 39 with permission). Solid points correspond to the 2 hour exposure reported in Ref. 39 and open points are from previous experiments at different exposure times also cited in Ref. 39.

5. The gap region between Be wall tiles depicting various zones and processes identified in the model by Kukushkin that can impact hydrogen deposition deep in the gaps. The D^+, C^{+n} arrow at the top denote income plasma ions streaming along the tilted magnetic field.

6. Raman spectra (relative intensities of the graphite-like mode, I_G, and disordered-like mode, I_D, are indicated) from (a) an unused NSTX tile, (b) dust from NSTX, (c) arc produced soot, and (d) both anode and cathode sides of a carbon sample ohmically heated to ~ 2500 °C.

7. Pictures of the surface of tungsten samples exposed to plasma and laser pulses show that synergistic effects of combined laser heat pulse and deuterium plasma cause greater surface roughening and material removal than with either by itself.

(a)

(b)

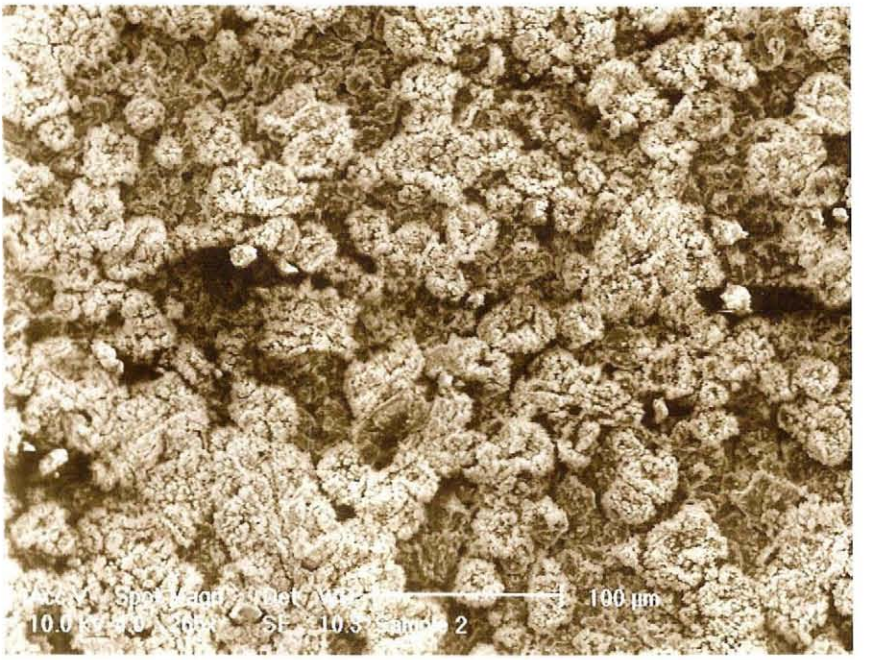

(c)

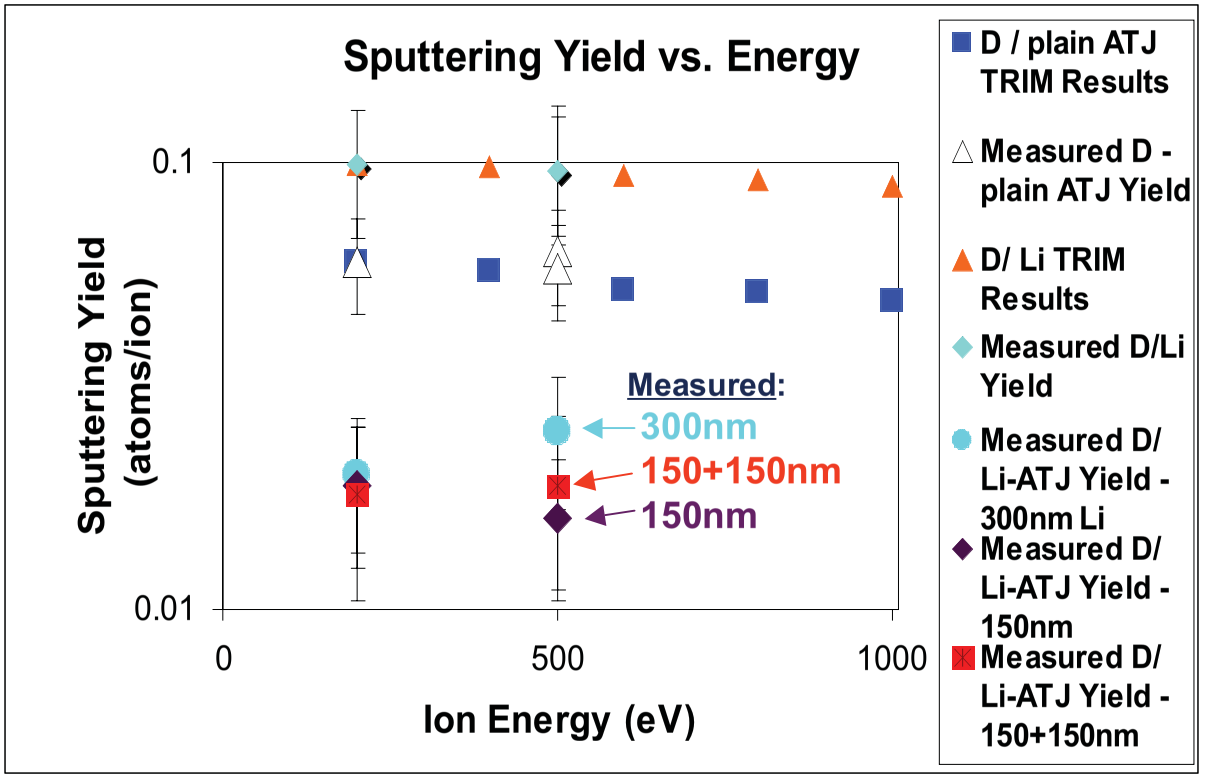
Sputtering Yield vs. Energy
Sputtering Yield (atoms/ion)
0.1
0.01
0
500
1000
Ion Energy (eV)
Measured:
300nm
150+150nm
150nm
D / plain ATJ TRIM Results
Measured D - plain ATJ Yield
D/ Li TRIM Results
Measured D/Li Yield
Measured D/ Li-ATJ Yield - 300nm Li
Measured D/ Li-ATJ Yield - 150nm
Measured D/ Li-ATJ Yield - 150+150nm

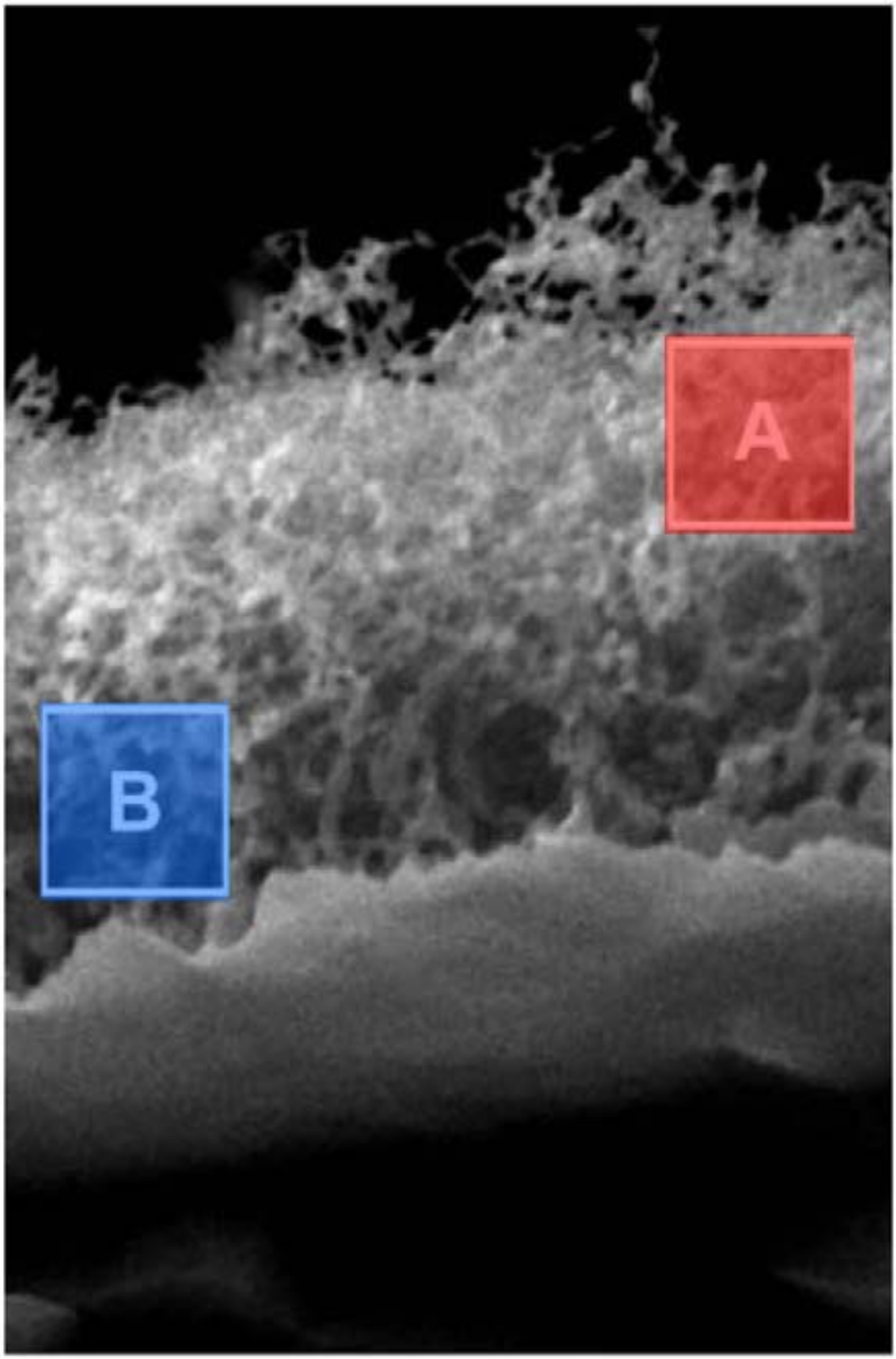
A
B
X30,000 0.5µm
UC PISCES

(a)

Present
673 K
623 K

Previous [10]
623 K
573 K
523 K

(Remaining D content) x10^{22} (D m^{-2})

1

0.1

0.1
1
10
100

O_2 pressure (kPa)

(b)

Present
79 kPa
21 kPa
2.1 kPa

Previous [10]
21 kPa
2.1 kPa
0.21 kPa

1

0.1

550
600
650
700

Temperature (K)

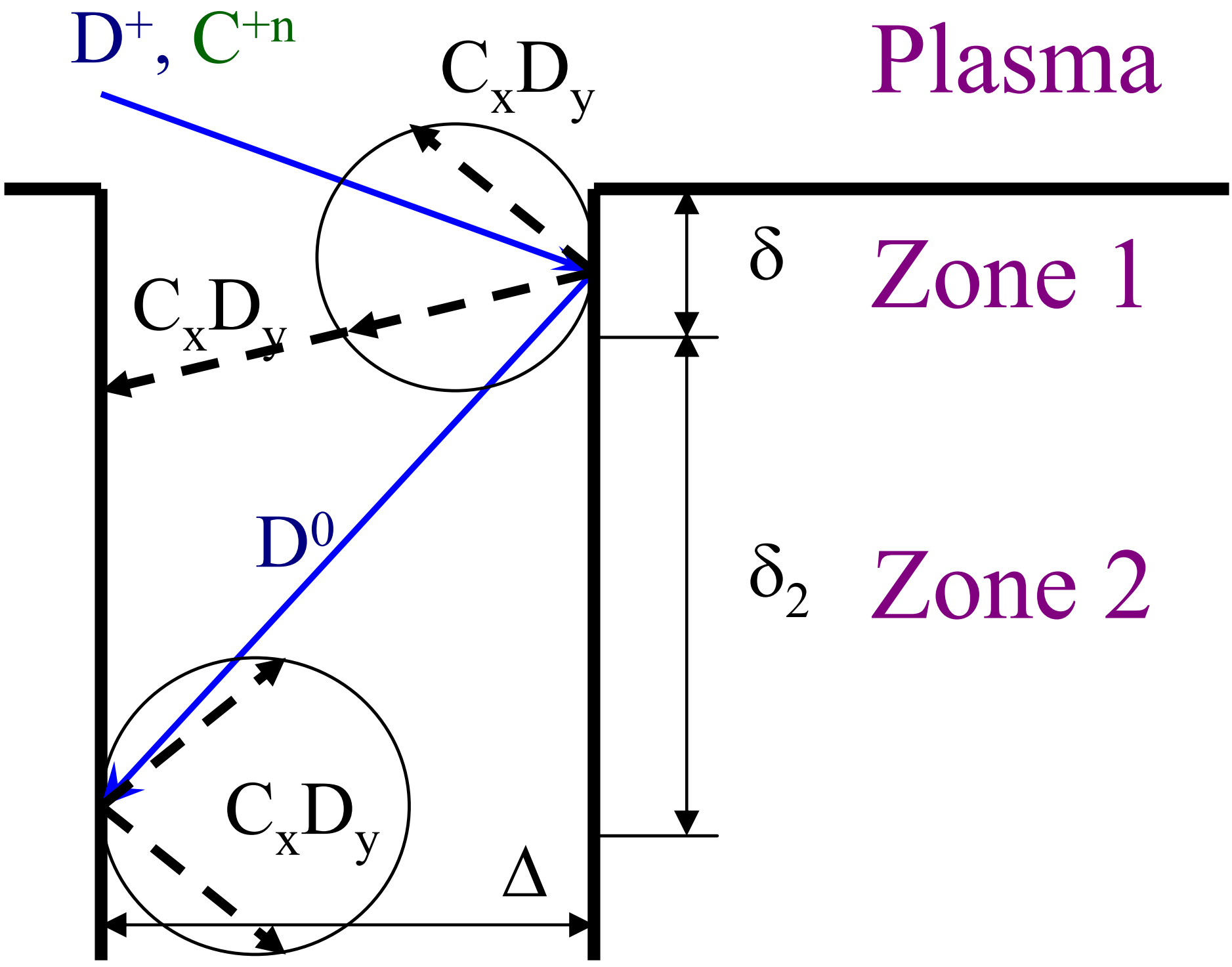
D+, C+n
CxDy
Plasma
δ
Zone 1
CxDy
D0
δ2
Zone 2
CxDy
Δ

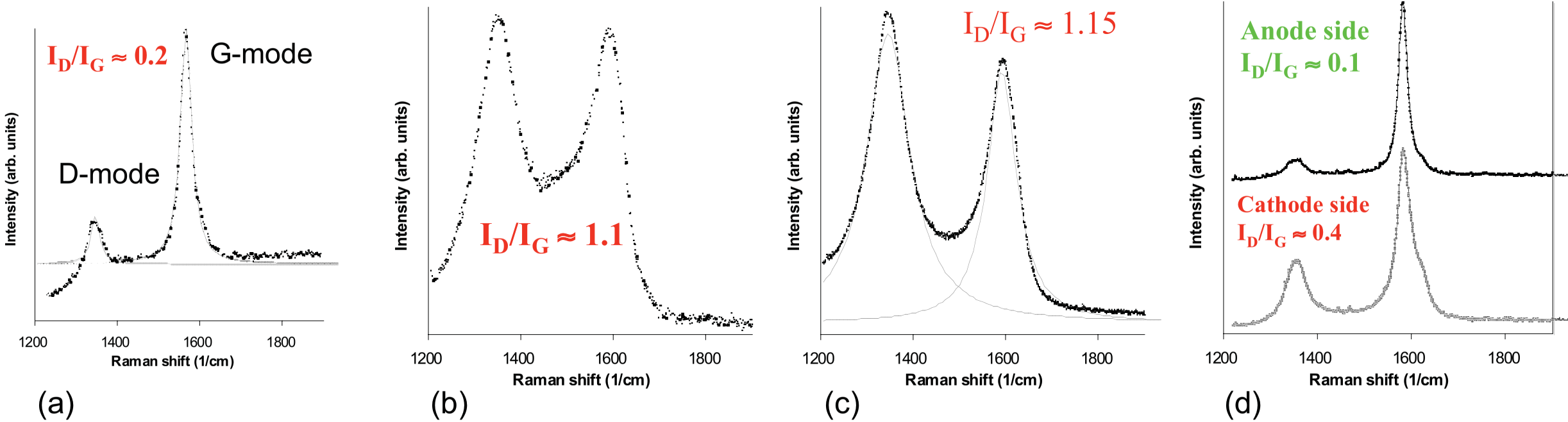
$I_D/I_G \approx 0.2$
G-mode
D-mode
Intensity (arb. units)
1200
1400
1600
1800
Raman shift (1/cm)
(a)
$I_D/I_G \approx 1.1$
Intensity (arb. units)
1200
1400
1600
1800
Raman shift (1/cm)
(b)
$I_D/I_G \approx 1.15$
Intensity (arb. units)
1200
1400
1600
1800
Raman shift (1/cm)
(c)
Anode side
$I_D/I_G \approx 0.1$
Cathode side
$I_D/I_G \approx 0.4$
Intensity (arb. units)
1200
1400
1600
1800
Raman shift (1/cm)
(d)

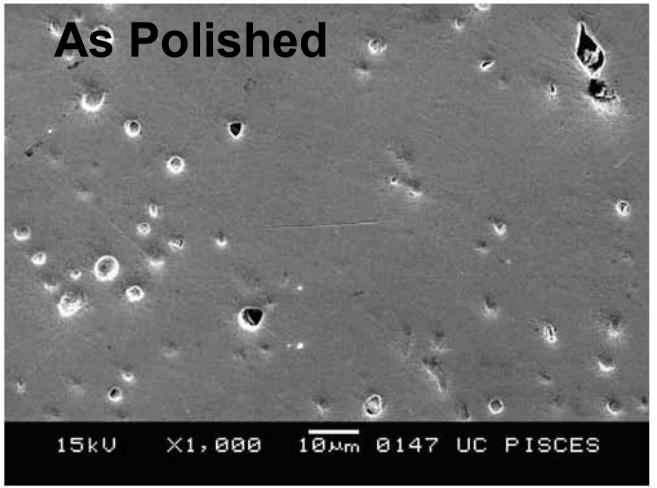
As Polished
15kV X1,000 10µm 0147 UC PISCES

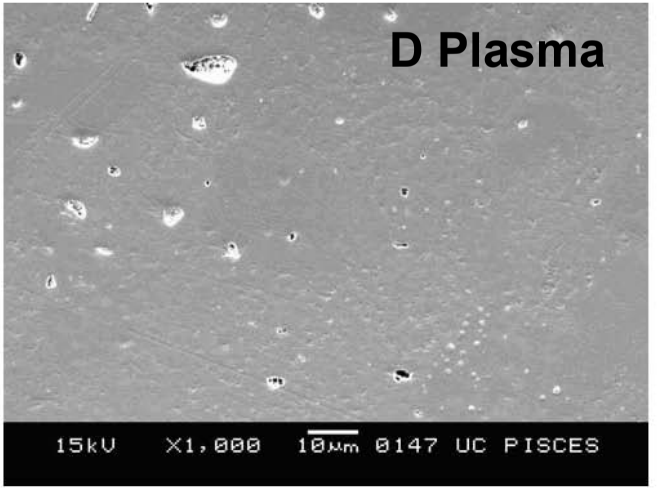
D Plasma
15kV X1,000 10µm 0147 UC PISCES

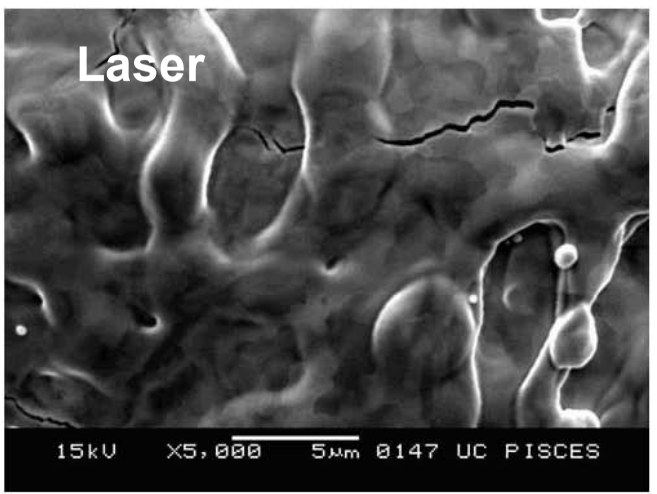
Laser
15kV X5,000 5µm 0147 UC PISCES

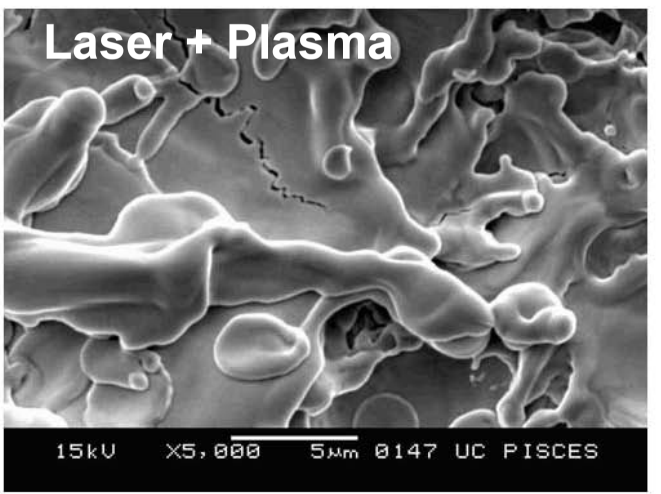
Laser + Plasma
15kV X5,000 5µm 0147 UC PISCES

The Princeton Plasma Physics Laboratory is operated
by Princeton University under contract
with the U.S. Department of Energy.

Information Services
Princeton Plasma Physics Laboratory
P.O. Box 451
Princeton, NJ 08543

Phone: 609-243-2750
Fax: 609-243-2751
e-mail: pppl_info@pppl.gov
Internet Address: http://www.pppl.gov